Small-Sized MMIC Amplifiers Using Thin Dielectric Layers

Seiichi Banba, *Member, IEEE,* and Hiroyo Ogawa, *Member, IEEE*

***Abstract*—Miniaturized MMIC amplifiers utilizing a multilayer structure composed of thin film transmission lines are presented. The fundamental characteristics of the thin film transmission lines for use in microwave active circuits are discussed through calculations by numerical analysis. A two-stage low-noise amplifier, a single-stage wideband amplifier, and a balanced amplifier are designed within very small areas, while good performance is maintained. The results include that a Ka-band single-stage amplifier is fabricated in a 0.8 mm× 0.6 mm areas with a gain of 8.0–9.5 dB in the frequency range of 16–26.5 GHz and input/output return losses of better than 8 dB at 26.5 GHz. The proposed amplifier configurations can be applied to high density integration of one-chip MMIC modules.**

I. Introduction

MONOLITHIC microwave integrated circuits (MMIC's), which will be essential components in future communication systems, must be miniaturized. Large-scale complicated MMIC's are also required [1]. Fortunately, a thin film transmission line structure, which utilizes narrow-width microstrip conductors on thin (several-μm-thick) dielectric materials fabricated over a ground plane metal on a GaAs wafer surface, was recently reported [2]–[6]. Thin film transmission lines allow for high density circuit integrations due to reduced transmission line widths and their ready application to multilayer configurations. For example, thin film transmission lines such as microstrip, inverted microstrip, and triplate lines can be applied to a multilayered transmission line structure using a ground plane metal, which serves to separate the transmission lines [7]. In addition, meander-like and cross-over transmission line structures are easily fabricated in a small area. Therefore, a highly flexible circuit design is achieved for a 3-dimensional structure, and this configuration can be used for high density integration of MMIC's. Thin film transmission lines can also be integrated within uniplanar microwave circuits [8]. Monolithic microwave integrated circuits using thin film transmission lines are usually called multilayer MMIC's. Several microwave passive circuits using thin film transmission lines have been reported [2]–[4], [7].

Manuscript received January 17, 1994; revised June 29, 1994.

S. Banba was with ATR Optical and Radio Communications Research Laboratories, Kyoto 619-02, Japan. He is now with SANYO Electric Co., Ltd., Osaka 573, Japan.

H. Ogawa was with ATR Optical and Radio Communications Research Laboratories. He is now with NTT Radio Communication Systems Laboratories, Yokosuka-shi 238-03, Japan.

IEEE Log Number 9407440.

However, design methods and applications for active circuits such as amplifiers and mixers have not been sufficiently discussed. Although thin film transmission lines can substantially reduce the circuit area, they show relatively high insertion losses compared to conventional microwave transmission lines such as microstrip and coplanar waveguide lines, and degrade circuit performance [4]. It is therefore important to optimize the structure of the transmission lines in the MMIC design.

In this paper, the fundamental characteristics of thin film transmission lines are calculated by the quasi-static and full-wave finite-element method (FEM), and their suitability for use in microwave active circuits is demonstrated. A design method that allows reducing the circuit area and obtaining good performance is presented using numerical results and an equation. Thin film transmission line structures, that is, microstrip line, inverted microstrip line, and triplate line structures using polyimide films as thin dielectric substrates are successfully utilized to realize miniaturized MMIC amplifiers. An X-band two-stage low-noise amplifier, a Ka-band single-stage wideband amplifier, and a balanced amplifier are fabricated utilizing these transmission line structures, and their performance is also demonstrated. The intrinsic circuit area of the amplifiers is about one-fourth that of conventional MMIC's.

II. Thin Film Transmission Lines

The fundamental characteristics of microstrip, inverted microstrip, and triplate lines using thin dielectric layers are discussed in this section. A schematic cross-sectional view of these transmission lines [6] is shown in Fig. 1. Each transmission line is formed on a GaAs wafer surface. These structures consist of polyimide films for the thin dielectric layers and 1-μm-thick gold films for the conductor metals. A process for polyimide film preparation and subsequent chemical etching is reported in [9]. This process can generate cone-shaped via-holes, which connect the microstrip conductors on the upper dielectric layers with the input/output ports and microstrip conductors on the lower dielectric layers. The relative dielectric constant and loss tangent of the polyimide film are 3.7 and 0.01 (10 MHz), respectively. A uniformity in the film thickness of better than 1% is obtained up to 10 μm. The measured stress of the polyimide film is a constant value of -2.4×10^8 dyn/cm^2, and is one-tenth that of Si_3N_4 and SiO_2 films. Furthermore, the surface of the film, which is formed by spin-coating, is flat due to its high viscosity. These

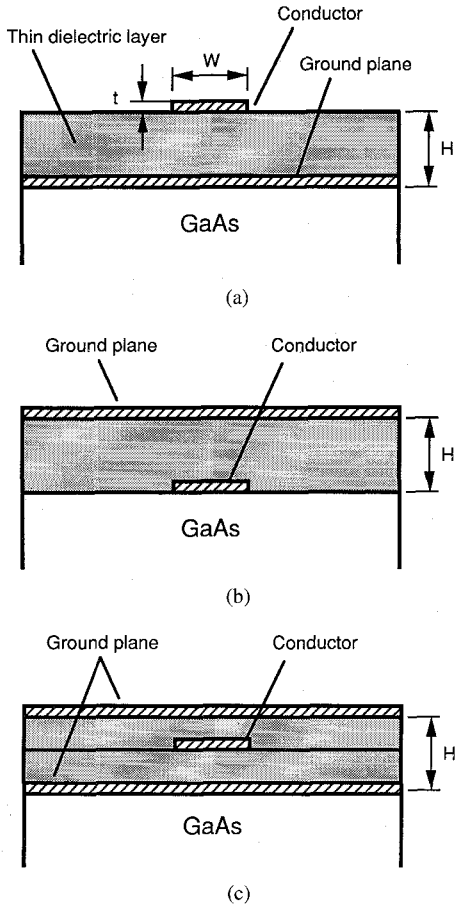

Fig. 1. Basic transmission line structures using thin dielectric layers. (a) A microstrip line structure. (b) An inverted microstrip line structure. (c) A triplate line structure.

properties show the polyimide film to be a suitable dielectric material for thin film transmission line fabrication, and the polyimide film has excellent reliability for GaAs devices [10]. In our fabrication, the multilayer structure consists of two 5.0-μm-thick polyimide films to construct a three-layer conductor.

The calculated characteristic impedance and normalized guided wavelength (λ_g/λ_o) of these transmission lines are shown in Fig. 2. Because these structures are small in comparison to their guided wavelength, quasi-TEM approximation can be used for numerical analysis. For the inverted microstrip line and triplate line, the polyimide film flatness over the strip conductor, $\delta(N)$, must be considered, because the film thickness is somewhat decreased due to the presence of the lower conductor. The polyimide film flatness is given by the following equation:

$$\delta(N) = \left\{1 - \left(\frac{A}{B}\right)^N\right\} \times 100 \quad [\%] \tag{1}$$

where A, B, and N are the ramp height after polyimide formation, initial conductor thickness, and number of layer piles, respectively. According to our polyimide preparation conditions, the flatness of the first and second polyimide layers

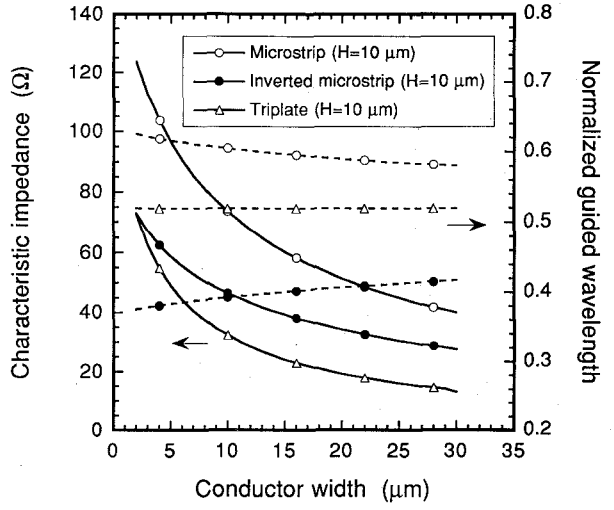

Fig. 2. Calculated characteristic impedance (solid line) and normalized guided wavelength (dashed line: λ_g/λ_o) of various transmission lines as a function of conductor width.

is 36% and 60%, respectively. The conductor widths of these transmission lines, whose characteristic impedances range from approximately 100–15 Ω, are between 5 and 30 μm, and are similar to the polyimide film thickness. Furthermore, the conductor widths of these transmission lines are less than one-fifth those of the microstrip lines in conventional MMIC's. Therefore, a highly flexible circuit design can be achieved. The conductor widths of the microstrip, inverted microstrip, and triplate lines, whose characteristic impedance is approximately 50 Ω, are 21, 8, and 5 μm, respectively, when the total polyimide film thickness is 10 μm. Since the inverted microstrip line has a relatively high effective dielectric constant due to the GaAs substrate, the conductor width is 40% less than that of a microstrip line. The triplate line has a low characteristic impedance with a narrow conductor width. This result shows the triplate line to be a suitable structure for a low impedance line in amplifier circuits, compared to the other two. For example, the conductor width of a 20-Ω triplate line ($H = 10$ μm) is only approximately 20 μm. An application of low-characteristic impedance lines as impedance transformers was reported in [11].

III. Losses in Thin Film Transmission Lines

Thin film transmission lines show relatively high insertion losses, dominated by conductor losses, due to narrow widths of the microstrip conductors. The conductor losses (at 20 GHz) of these transmission lines are calculated by full-wave FEM [12]. In the calculation, the skin effect is considered, because the conductor thickness is approximately two times greater than the skin depth of the conductor at 20 GHz. We also assume the surface roughness of the conductor to be zero, from observations by scanning electron microscopy (SEM). The calculated conductor losses of 50-Ω microstrip line structures as a function of the polyimide film thickness are shown in Fig. 3. The calculated results show that the conductor losses of the transmission lines decrease rapidly with increasing polyimide film thickness, and range from

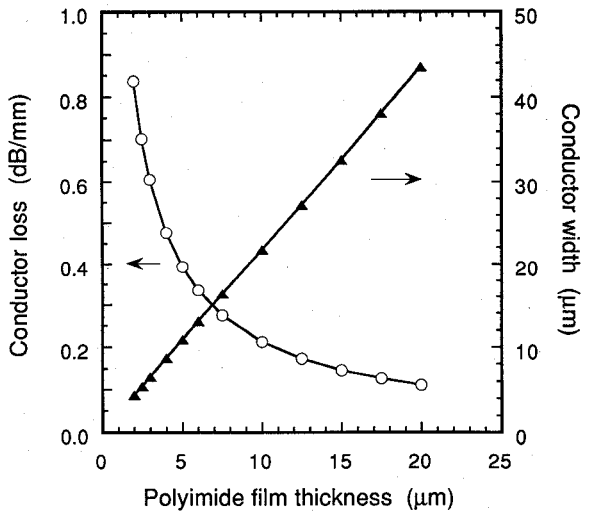

Fig. 3. Calculated conductor loss and conductor width of 50-Ω microstrip lines as a function of polyimide film thickness at a frequency of 20 GHz.

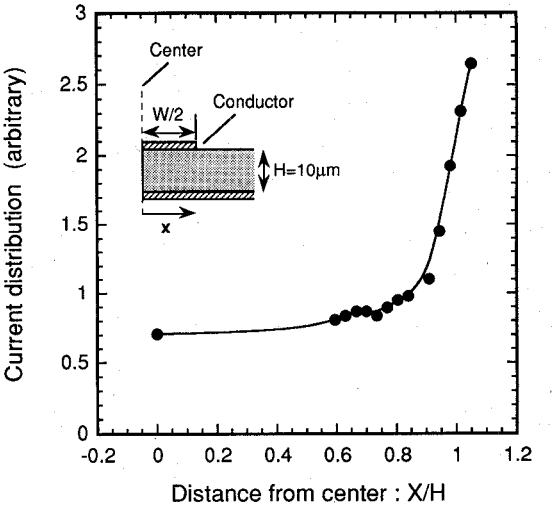

Fig. 5. Current distribution for the symmetrical half space of a microstrip line ($H = 10$ μm, $W = 21$ μm, $W/H = 2.1$).

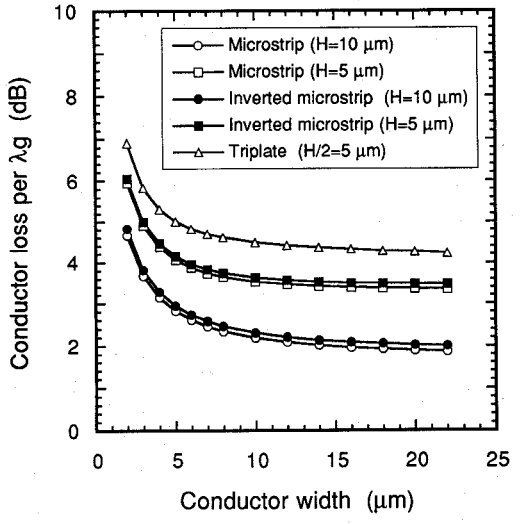

Fig. 4. Calculated conductor loss (per λ_g) of various transmission lines as a function of conductor width at a frequency of 20 GHz.

0.84–0.11 dB/mm for thicknesses of 2–20 μm; they show smaller improvements above 10 μm. The conductor losses of these transmission lines as a function of the conductor width, assuming polyimide thicknesses of 10 and 5 μm, are shown in Fig. 4. The calculated current distribution for the symmetrical half space of a microstrip line is shown in Fig. 5. The current concentrates near both edges of the microstrip conductor, and rapidly decreases for distances from the conductor edge up to 2.5 μm ($x/H = 0.25$). Therefore, the conductor losses of these transmission lines are slightly reduced for conductor widths of above 5 μm ($= H/2$). To reduce the transmission line loss, the thickness of the polyimide film and conductor width must be greater than 5 μm. Transmission lines having identical conductor widths and polyimide thicknesses show almost the same insertion losses (per λ_g) for different characteristic impedances. For example, a 50-Ω microstrip line and a 35- Ω inverted microstrip line with the same conductor width ($W =$ 10 μm) have almost the same insertion loss (per λ_g), when the polyimide film thickness is 5 μm, as shown in Fig. 4.

Losses in the microstrip line have been discussed in [2], [13], and [14]. To calculate the circuit performance, we must simulate the frequency characteristic of the transmission line attenuation with a commercially available CAD software package. The surface resistivity R_s which is considered as the skin effect [2] is given by (2)

$$R_s(f) = R_{so}tK \cdot \sqrt{f}/(1 - e^{-tK\sqrt{f}}) \quad [\Omega/\square] \qquad (2)$$

where t and K are the conductor thickness and material constant ($= \sqrt{\pi\sigma\mu}$), respectively. The conductor loss α_c is proportional to R_s

$$\alpha_c(f)/\alpha_c(F) = R_s(f)/R_s(F) \qquad (3)$$

where f and F are the operating frequency and defined frequency, respectively. The dielectric loss $\alpha_d(f)$ is estimated by using the following assumptions [15]: 1) the loss tangent of the polyimide film is proportional to the operating frequency, and 2) the value of the loss tangent is 0.020 at 20 GHz:

$$\tan\delta(f)/\tan\delta(F) = f/F \qquad (4)$$

$$\alpha_d(f) = \frac{27.3}{\lambda_g}\tan\delta(f) = 27.3 \cdot \frac{f}{c} \cdot \sqrt{\epsilon_{\text{eff}}} \cdot \tan\delta(f) \quad [\text{dB/mm}]. \qquad (5)$$

Therefore, in the circuit design, the frequency characteristic of the total attenuation per unit length $\alpha(f)$ is given by the following equation, rewriting the calculated or evaluated value, $\alpha_c(F)$ or $\alpha_d(F)$, at a design frequency of F (in our case,

TABLE I
STRUCTURAL PARAMETERS AND CHARACTERISTICS OF THIN FILM TRANSMISSION LINES FOR USE IN AMPLIFIERS THE LOSSES ARE CALCULATED AT 20 GHz

	Structure	Line width [μm]	Polyimide thickness [μm]	Characteristic impedance [Ω]	Effective dielectric constant	Conductor loss [dB/mm]
(a)	Microstrip line	10	10	75.0	2.73	0.241
(b)	Microstrip line	10	5	50.0	2.87	0.398
(c)	Inverted microstrip line	10	5	35.0	6.04	0.590
(d)	Triplate line	14	10	25.0	3.70	0.559
(e)	Input / output CPW-port	Width / Gap = 42 / 29	---	50.0	6.83	0.093
(f)	CPW	Width / Gap = 12 / 10	---	50.0	6.54	0.278

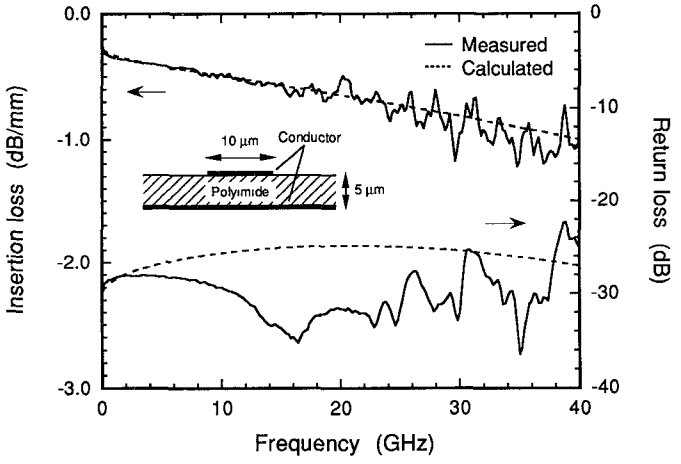

Fig. 6. Calculated and measured frequency characteristics of a 50-Ω microstrip line ($H = 5$ μm, $W = 10$ μm). Solid line: measured; dashed line: calculated.

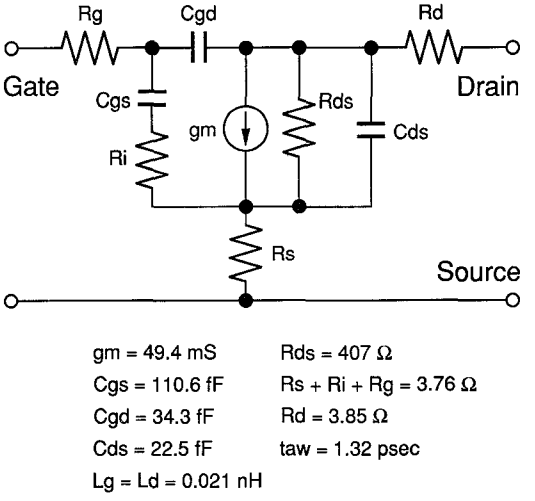

Fig. 7. Small-signal equivalent circuit of a HEMT with a 100 μm width and 2-finger gate ($V\,ds = 3$ V, $I\,dss = 20$ mA).

$F = 20$ GHz):

$$\alpha(f) = \alpha_c(F) \cdot \sqrt{\frac{f}{F}} \cdot \frac{1 - e^{-tK\sqrt{F}}}{1 - e^{-tK\sqrt{f}}} + \alpha_d(F) \cdot \frac{f^2}{F^2} \quad \text{[dB/mm]}. \quad (6)$$

The transmission lines, whose structural parameters are summarized in Table I, are tested using on-wafer probes and an HP8510 network analyzer. The length of the measured transmission lines with coplanar waveguide (CPW) ports is 1.3 mm (intrinsic line length: 1.0 mm). Each transmission line is connected to the CPW-ports through via-holes (15 μm × 15 μm) on the GaAs wafer surface, and the transition loss between every CPW-port and transmission line is less than 0.075 dB at 20 GHz. Fig. 6 shows the calculated and measured characteristics of a microstrip line (type (b) in the Table I). A good agreement between these values is obtained in the frequency range of 0–40 GHz using (6).

IV. AMPLIFIER DESIGN AND PERFORMANCE

An AlGaAs/InGaAs pseudomorphic HEMT with a T-shaped 0.25-μm gate is applied to the amplifier circuits. The gate width and gate finger number of the HEMT are 100 μm and 2, respectively. The HEMT has a calculated cutoff frequency of 45 GHz, and its small-signal equivalent circuit is determined from S-parameter measurements up to 40 GHz as shown in Fig. 7. The noise parameters are characterized by using an on-wafer noise measurement system up to 18 GHz. The values of the noise figure, Γ_{opt} and Rn are 1.05 dB, 0.571 ∠43.2°, and 19.1 Ω, respectively, at 12 GHz.

In the circuit design, we adopt a commercially available CAD software package, which includes a user defined function routine (Touchstone), to optimize circuit parameters by using (6) for the frequency characteristics of the transmission lines. Each transmission line has a meander-like configuration, and short-stub lines are arranged over MIM (metal-insulator-metal) bypass capacitors to reduce the circuit area; each line is connected to the upper metal of the capacitors through via-holes. Table I summarizes the structural parameters and calculated performance of the transmission lines in the fabricated amplifiers. For reference, values from conventional CPW structures are also shown. The conductor widths of these transmission lines are less than 14 μm, and the gap of the strip conductors is about four times the conductor width and the dielectric thickness; therefore, the

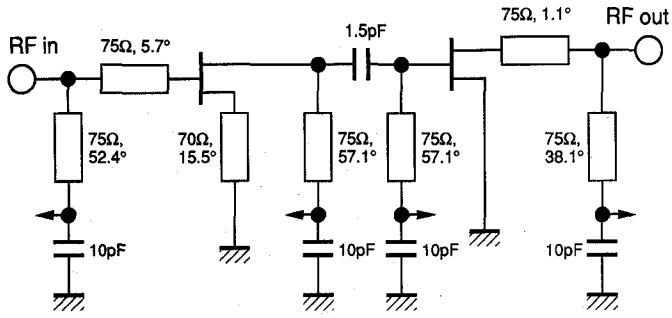

(a)

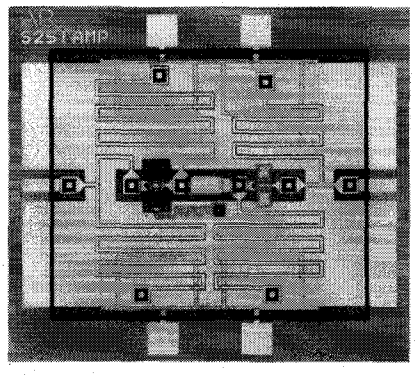

(b)

Fig. 8. (a) Circuit diagram and (b) photograph of an X-band LNA (chip size: 1.2 mm × 1.08 mm). The electrical lengths of the transmission lines are given at 12 GHz.

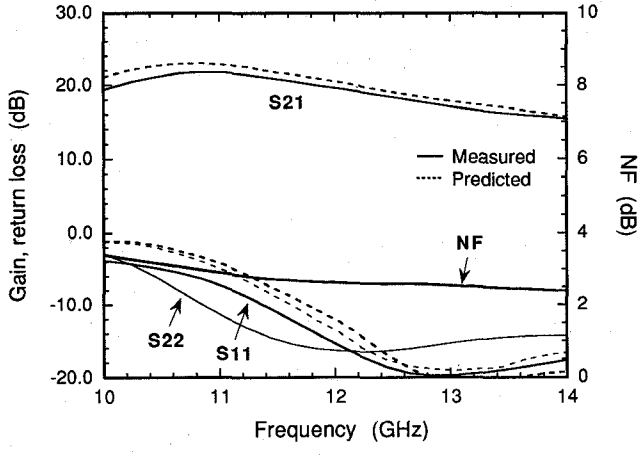

Fig. 9. Characteristics of fabricated X-band LNA. ($V\,ds = 3$ V, $I\,dss =$ 20 mA). Solid line: measured; dashed line: predicted.

coupling effect of the transmission lines is almost eliminated.

An X-band two-stage LNA, integrated with two HEMT's, four 10-pF capacitors, and a 2-pF capacitor as lumped elements, is fabricated using a microstrip line structure. The circuit diagram and a photograph of the LNA are shown in Fig. 8. The intrinsic circuit area is 0.80 mm × 0.78 mm, and is one-fourth that of conventional MMIC's [16]. The first-stage HEMT has a source feedback inductance to achieve the optimum noise matching [17]. The matching network is designed employing six 75-Ω microstrip lines and a 70-Ω microstrip line for the source feedback inductance. Both transmission lines are formed on different dielectric layers to obtain a flexible layout. The measured and calculated characteristics of the two-stage amplifier are shown in Fig. 9. The noise performance of the fabricated amplifier is measured using an on-wafer probe station and an HP8970 noise figure meter. The amplifier shows a noise figure of 2.6–2.65 dB and a gain of 19.1–20.3 dB in the frequency range of 11.7–12.2 GHz, and its input/output VSWR's are better than 1.6 and 1.4, respectively. To obtain approximately 20-dB gain, a current dissipation of 20 mA is required for each HEMT. (In high-power applications, a process for removing the polyimide films over the transistors or an additional thermal treatment (more than 185°C or up to 350°C) is needed to maintain the thermal stability of the polyimide films.) The noise performance is slightly deteriorated in comparison to the conventional MMIC's. Excess value of the noise figure caused by transmission line losses is approximately 0.95 dB at 12 GHz. Fig. 10 shows the output power of the fundamental and third-order intermodulation products as a function of the input power. The frequencies of the input signals are 12.00 and 12.04 GHz. The 1-dB compression point ($P_{1\,dB}$) and third-order intercept point (IP_3) are 6 and 16 dBm, respectively.

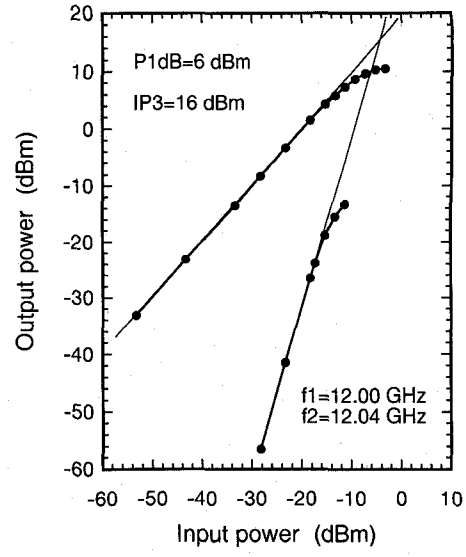

Fig. 10. Output power of the fundamental and third-order intermodulation products as a function of input power.

A Ka-band single-stage wideband amplifier is designed for a center frequency of 20 GHz. The circuit diagram and a photograph of the amplifier are shown in Fig. 11. The impedance of the transmission lines is constrained to be within the range of 20–80 Ω, for the purposes of a reduced size and an acceptable transmission line loss. Low impedance, less than 30 Ω, transmission lines, which are difficult to utilize in conventional MMIC's, are chosen to achieve amplifier gain flatness in a wide band. In this case, a triplate line is used as the 25-Ω transmission line, and a microstrip line is used as the 75-Ω transmission line. Fig. 12 shows the calculated and measured amplifier performance. The ampli-

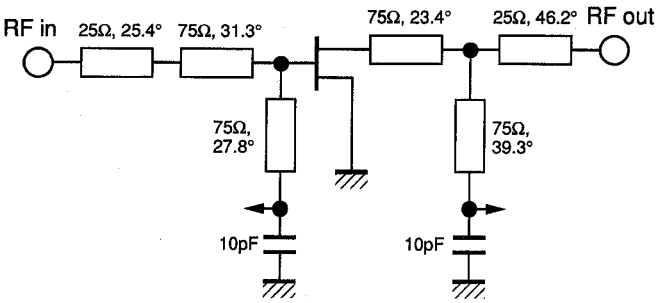

(a)

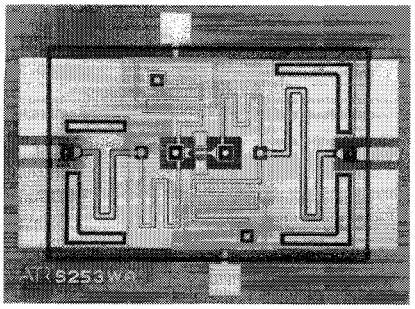

(b)

Fig. 11. (a) Circuit diagram and (b) photograph of a single-stage wideband amplifier (chip size: 1.2 mm × 0.9 mm). The electrical lengths of the transmission lines are given at 20 GHz.

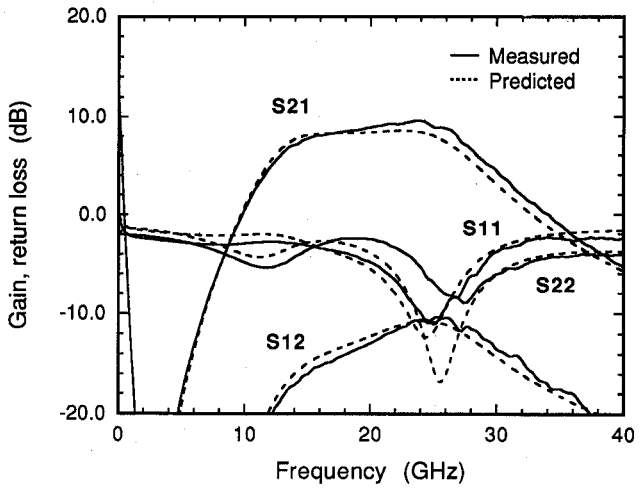

Fig. 12. Characteristics of fabricated wideband amplifiers ($V\,ds$ = 3 V, $I\,dss$ = 20 mA). Solid line: measured; dashed line: predicted.

fier shows a gain of 8.0–9.5 dB in the frequency range of 16.0–26.5 GHz, and its input/output return losses are better than 8 dB at 26.5 GHz. The amplifier also shows a noise figure of 4.6–5.2 dB, and its noise characteristics are slightly deteriorated due to lossy transmission lines. However, the chip size is 1.2 mm × 0.9 mm, while the intrinsic circuit area is only 0.8 mm × 0.6 mm. This amplifier circuit is applied to a unit-amplifier of a balanced amplifier as described below.

To demonstrate the ability of the multilayer structure, we designed a balanced amplifier [18] at a center frequency of 20 GHz using branch-line hybrids, as 90-degree couplers, com-

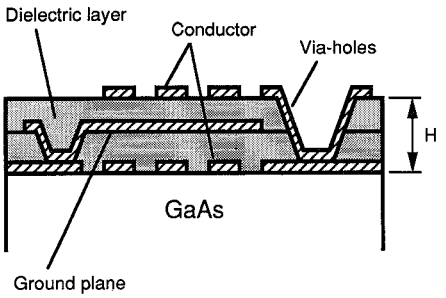

(a)

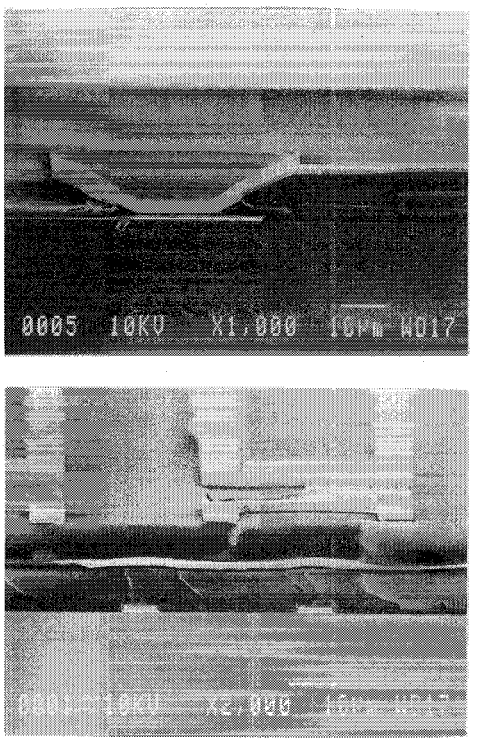

(b)

Fig. 13. Multilayer transmission line structure using two dielectric layers. (a) Schematic cross-section and (b) SEM photographs of a fabricated structure (multilayered transmission lines and a via-hole view).

posed of a multilayer structure. A schematic cross-sectional view of the multilayer structure and SEM photographs of a fabricated hybrid, similar to [7], are shown in Fig. 13. The hybrid shows coupling losses of 5.4 dB ± 0.3 dB, and return losses and isolation of better than 15 dB in the frequency range of 18–22 GHz. The circuit diagram and a photograph of a balanced amplifier MMIC are shown in Fig. 14. The intrinsic circuit area is 1.09 mm × 1.54 mm, although the balanced amplifier is constructed with two branch-line hybrids and two amplifiers. Fig. 15 shows the measured and calculated characteristics of the balanced amplifier. The fabricated balanced amplifier shows a gain of 5.5 dB with a 3 dB-bandwidth of 4 GHz, and its input/output return losses are better than 20 dB at a center frequency of 20 GHz. To obtain improved performance without increasing the circuit area, it is necessary to reduce the excess coupling loss of the

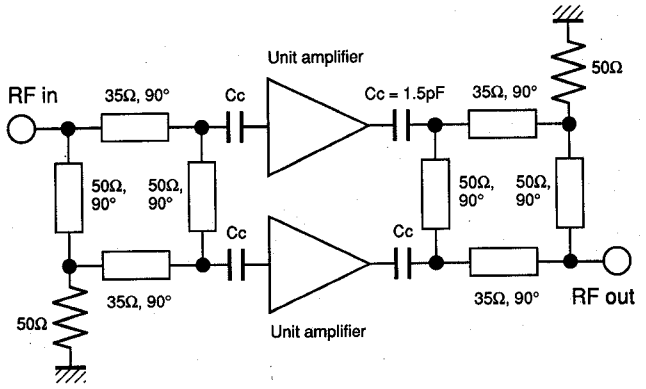

(a)

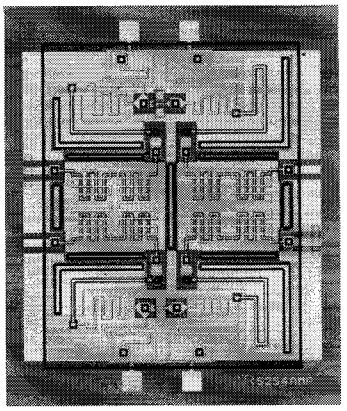

(b)

Fig. 14. (a) Circuit diagram and (b) photograph of a balanced amplifier (chip size: 1.49 mm × 1.84 mm). The electrical lengths of the transmission lines are given at 20 GHz.

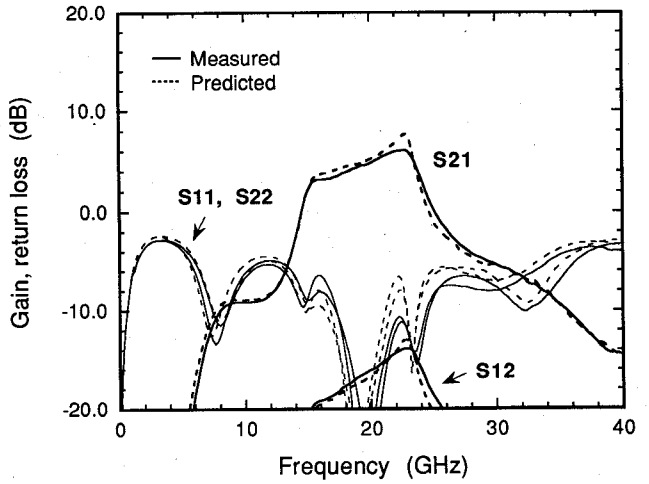

Fig. 15. Characteristics of a fabricated balanced amplifier ($V\,ds = 3$ V, $I\,dss = 20$ mA). Solid line: measured; dashed line: predicted.

90-degree hybrid. Investigations for new types of hybrids are in progress.

V. Conclusion

Very small-sized MMIC amplifiers using thin film transmission line structures composed of thin dielectric layers on the GaAs wafer surface have been proposed, and their performance was demonstrated. The transmission line structures can be effectively combined with microwave active circuits. An X-band two-stage LNA, a Ka-band single-stage wideband amplifier, and a balanced amplifier have been designed within very small areas, e.g., 0.63 mm^2, 0.48 mm^2, and 1.68 mm^2, respectively, while good performance has been maintained. The proposed amplifier configurations can be applied to high-density and multifunctional integration of MMIC modules.

VI. Acknowledgment

The authors would like to thank Dr. K. Habara, Dr. H. Inomata, and Dr. E. Ogawa of ATR Optical and Radio Communications Research Laboratories for their continuous support and encouragement. The authors also wish to thank Dr. Y. Harada, K. Nagami, and T. Yamada of SANYO Electric Co. Ltd. for their help in fabricating the MMIC's.

References

[1] J. Berenz, M. LaCon, and M. Luong, "Single chip Ka-band transceiver," in *Proc. IEEE MTT-S Int. Microwave Symp.*, June 1991, pp. 517–520.

[2] T. Hiraoka, T. Tokumitsu, and M. Aikawa, "Very small wide-band MMIC magic-T's using microstrip lines on a thin dielectric film," *IEEE Trans. Microwave Theory Tech.*, vol. MTT-37, pp. 1569–1575, Oct. 1989.

[3] H. Nakamoto, T. Tokumitsu, and M. Aikawa, "A monolithic, port-interchanged rat-race hybrid using a thin film microstrip line crossover," in *Proc. 19th European Microwave Conf.*, Sept. 1989, pp. 311–316.

[4] T. Tokumitsu, T. Hiraoka, H. Nakamoto, and T. Takenaka, "Multilayer MMIC using a 3 μm × 3-layer dielectric film structure," in *Proc. IEEE MTT-S Int. Microwave Symp.*, May 1990, pp. 831–834.

[5] H. Ogawa, T. Hasegawa, S. Banba, and H. Nakamoto, "MMIC transmission lines for multi-layered MMIC's," in *Proc. IEEE MTT-S Int. Microwave Symp.*, June 1991, pp. 1067–1070.

[6] S. Banba, T. Hasegawa, H. Ogawa, and T. Tokumitsu, "Novel MMIC transmission lines using thin dielectric layers," *IEICE Japan Trans. Electron.*, vol. E75-C, pp. 713–720, June 1992.

[7] S. Banba, T. Hasegawa, and H. Ogawa, "Multilayer MMIC branch-line hybrid using thin dielectric layers," *IEEE Microwave and Guided Wave Lett.*, vol. 1, pp. 346–347, Nov. 1991.

[8] T. Hirota, Y. Tarusawa, and H. Ogawa, "Uniplanar MMIC hybrid—A proposed new MMIC structure," *IEEE Trans. Microwave Theory Tech.*, vol. MTT-35, pp. 576–581, June 1987.

[9] Y. Harada, F. Matsumoto, and T. Nakakado, "A novel polyimide film preparation and its preferential-like chemical etching techniques for GaAs device," *J. Electrochem. Soc.*, vol. 130, pp. 129–134, Jan. 1983.

[10] Y. Harada and K. Honda, "Reliability of beam leaded GaAs microwave devices fabricated by using thick polyimide film," in *Proc. 172nd Fall Meet. Electrochem. Soc.*, Honolulu, HI, 1987, pp. 652–655.

[11] M. Gillick and I. Robertson, "X-band monolithic power amplifier using low characteristic impedance thin film microstrip transformers," *IEEE Microwave and Guided Wave Lett.*, vol. 2, pp. 328–330, Aug. 1992.

[12] M. Matsuhara and T. Angkaew, "Analysis of waveguide with loss or gain by the finite-element-method," *Trans. IEICE*, vol. J71-C, pp. 1398–1403, Oct. 1988.

[13] K. C. Gupta, R. Garg, and I. J. Bahl, *Microstrip Lines and Slotlines.* Norwood, MA: Artech House, 1979.

[14] R. A. Pucel, D. J. Masse, and C. P. Hartwig, "Losses in microstrip," *IEEE Trans. Microwave Theory Tech.*, vol. MTT-16, pp. 342–350, June 1968.

[15] Y. Pastol, G. Arjavalingam, J. M. Halbout, and G. V. Kopcsay, "Absorption and dispersion of low-loss dielectrics measured with microwave transient radiation," *Electron. Lett.*, vol. 25, pp. 523–524, Apr. 1989.

[16] B. Hughes, J. Perdomo, and H. Kondoh, "12 GHz low-noise MMIC amplifier designed with a noise model that scales with MODFET size and bias," *IEEE Trans. Microwave Theory Tech.*, vol. 41, pp. 2311–2316, Dec. 1993.

[17] R. E. Lehmann and D. D. Heston, "X-band monolithic series feedback LNA," *IEEE Trans. Microwave Theory Tech.*, vol. MTT-33, pp. 1560–1566, Dec. 1985.
[18] R. S. Engelbrecht and K. Kurokawa, "A wide-band low noise L-band balanced transistor amplifier," *Proc. IEEE,* vol. 53, pp. 237–247, Mar. 1965.

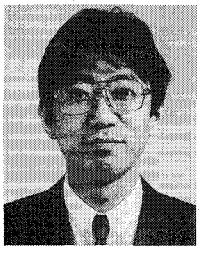

Seiichi Banba (M'91) received the B.S. and M.S. degrees in electrical and electronic engineering from Toyohashi University of Technology, Toyohashi, Japan, in 1982 and 1984, respectively.

In 1984 he joined the Microelectronics Research Center of SANYO Electric Co. Ltd., Osaka, Japan, where he did research and development work on microwave devices. From 1990 to 1993 he investigated optical/microwave monolithic integrated circuits for personal communication systems at ATR Optical and Radio Communications Research Laboratories. Since 1994 he has been researching microwave devices at SANYO Microelectronics Research Center.

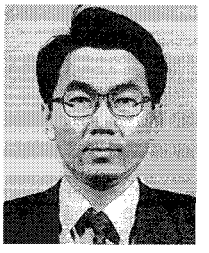

Hiroyo Ogawa (M'84) received the B.S., M.S., and Dr.Eng. degrees in electrical engineering from Hokkaido University, Sapporo, in 1974, 1976, and 1983, respectively.

He joined the Yokosuka Electrical Communication Laboratories, Nippon Telegraph and Telephone Public Corporation, Yokosuka, Japan, in 1976. He has been engaged in research on microwave and millimeter-wave integrated circuits, monolithic integrated circuits, and development of subscriber radio systems. From 1985 to 1986 he was a postdoctoral research associate at the University of Texas at Austin, on leave from NTT. From 1987 to 1988 he was engaged in the design of the subscriber ratio equipment at the Network System Development Center of NTT. From 1990 to 1992 he was engaged in the research of optical/microwave monolithic integrated circuits and microwave and millimeter-wave fiber optic links for personal communication systems at ATR Optical and Radio Communication Research Laboratories. Since 1993 he has been researching microwave and millimeter-wave photonics for communication satellites at NTT Radio Communication Systems Laboratories.

Dr. Ogawa is a member of the Institute of Electronics, Information, and Communication Engineers (IEICE) of Japan.